PROGRESSIVE DAMAGE IN WOVEN CFRPP IN PRESENCE OF SHOCK WAVES

R. Vignjevic[1*], N. Djordjevic[1], T. De Vuyst[1]

[1]*Department of Applied Mechanics and Astronautics, School of Engineering, Cranfield University, Cranfield, Bedfordshire, MK43 0AL, United Kingdom*
[2]*Institute, Department, University/Company, Address (Times New Roman 11 pt, Italic, left-aligned)*
**v.rade@cranfield.ac.uk*

Keywords: composites, thermo-elastic, shock wave, damage, hydrocode.

Abstract
The primary objective of the work presented in this paper was to develop a continuum thermoelastic-damage model for carbon fibre reinforced plastic (CFRP) materials, capable of modelling high rate deformation typical for ballistic impact loading. The constitutive model is capable of predicting formation and propagation of the shock waves in orthotropic materials and in addition can simulate damage initiation, evolution and failure. A key feature of the constitutive model is the decomposition of material volumetric and shear response. Material response under compression in this model is defined in terms of Mie Gruneisen equation of state (EOS) and the decomposition of stress tensor proposed in [1]. In order to take into account the orthotropy of the CFRP materials of interest, damage in this constitutive model is represented by a second order damage tensor $\boldsymbol{\omega}$*, which is incorporated in the stiffness tensor by using energy equivalence principle, see for instance [2]. Validation of the numerical model, implemented in LLNL DYNA3D [3], was done by the comparison of the numerical results to the experimental data obtained in the high velocity sphere impact tests published in [4]. The numerical results for the extent of damage were within 8% with the corresponding experimental data.*

1 Introduction
This paper describes development of the constitutive model, capable of predicting dynamic deformation and failure in the composites, which are widely used in aerospace and defense applications. Among the different architectures of the composite materials, the subject of this investigation is woven carbon-fibre reinforced plastic (CFRP) material, which can be conveniently modelled as an orthotropic (continuum) material.

The CFRP materials in the aerospace and defense applications are often exposed to the high rate impact loading, with the range of strain rates from $10^3\,s^{-1}$ to $10^6\,s^{-1}$. Typical impact scenarios are: debris impact, hail stone and ice impacts, bird strike, armour penetration etc. These extreme impact cases almost always involve generation and propagation of shock waves within the materials. Consequently, the material behaviour under such a complex loading need to be properly understood and accurately predicted, in order to optimise design of the structures and to minimise the risk of their catastrophic failure due to the impact hazards.

The thermoelastic damage model was developed in the framework of irreversible thermodynamics with internal variables. Due to the evident brittle properties of the composites, the elastic strains were assumed to be small and the plastic deformation was neglected (plastic deformation in CFRP considered does not exceed 1%). These assumptions significantly simplify the formulation of the constitutive model in the configurational and thermodynamic frameworks, in a way that it is derived in the current configuration and the dissipation of energy in the material during deformation process is induced by damage only.

2 Thermoelastic damage model

Damage in this constitutive model is represented by the second order damage tensor $\boldsymbol{\omega}$, which is incorporated into the elastic stiffness tensor of the damaged material via damage effect tensor $\mathbb{M}(\boldsymbol{\omega})$. This relationship is defined by using the principle of strain energy equivalence, originally derived by Cordebois and Sidoroff [5] as a generalization of pioneering work of Kachanov [6]. The damage effect tensor defines a linear relationship between the effective and nominal Cauchy stress tensors:

$$\bar{\boldsymbol{\sigma}} = \mathbb{M}(\boldsymbol{\omega}) : \boldsymbol{\sigma} \tag{1}$$

where $\bar{\boldsymbol{\sigma}}$ is effective Cauchy stress applied to the virgin material and $\mathbb{M}(\boldsymbol{\omega})$ is the fourth order damage effect tensor.

To maintain the symmetry of the effective stress tensor, the damage effect tensor is defined using the product type symmetrisation [7],[8], which is in the principle directions of damage defined as a fourth order diagonal tensor:

$$\mathbb{M}(\boldsymbol{\omega}) = (\mathbf{I} - \boldsymbol{\omega})^{-\frac{1}{2}} (\mathbf{I} - \boldsymbol{\omega})^{-\frac{1}{2}} \tag{2}$$

$$\mathbb{M}_{ijkl} = (\delta_{ik} - \omega_{ik})^{-\frac{1}{2}} (\delta_{jl} - \omega_{jl})^{-\frac{1}{2}} \tag{3}$$

where $\mathbf{I}$ is a second order identity tensor and δ_{ij} is Kronecker symbol.

Using the equivalence of complementary energy of damaged and virgin materials, combined with the definition of the damage effect tensor, given in the equations (1) to (3), the relationships between compliance and stiffness tensors of damaged and undamaged (virgin) materials are obtained in the following forms:

$$\mathbb{C}^{-1}(\boldsymbol{\omega}) = \mathbb{M}(\boldsymbol{\omega}) : \bar{\mathbb{C}}^{-1} : \mathbb{M}(\boldsymbol{\omega}) \tag{4}$$

$$\mathbb{C}(\boldsymbol{\omega}) = \mathbb{M}^{-1}(\boldsymbol{\omega}) : \bar{\mathbb{C}} : \mathbb{M}^{-1}(\boldsymbol{\omega}) \tag{5}$$

where $\mathbb{C}^{-1}$ and $\mathbb{C}$ are the compliance and stiffness tensors of the damaged material and $\bar{\mathbb{C}}^{-1}$ and $\bar{\mathbb{C}}$ are the compliance and stiffness tensors of the virgin material.

Compliance and stiffness tensors (4) and (5) can be used in the expression for thermodynamic state potentials, Helmholtz free energy and Gibbs free energy, and further in the definition of the dissipation rate [9]. Helmholtz free energy of the damaged material is defined per unit volume as:

$$\rho\psi\left(\boldsymbol{\varepsilon},\boldsymbol{\omega},\theta\right)=\frac{1}{2}\boldsymbol{\varepsilon}:\mathbb{C}:\boldsymbol{\varepsilon} \tag{6}$$

where ψ is specific free energy per unit mass, ρ is density, $\boldsymbol{\varepsilon}$ is strain tensor and θ is temperature.

Helmholtz free energy (6) can be transformed to the Gibbs free energy, making use of the Legendre transformation [9]:

$$\rho g\left(\boldsymbol{\sigma},\boldsymbol{\omega},\theta\right)=\rho\psi\left(\boldsymbol{\varepsilon},\boldsymbol{\omega},\theta\right)-\boldsymbol{\sigma}:\boldsymbol{\varepsilon}=-\frac{1}{2}\boldsymbol{\sigma}:\mathbb{C}^{-1}:\boldsymbol{\sigma} \tag{7}$$

where g is specific Gibbs free energy per unit mass.

Dissipation rate Δ is defined in terms of rate of change of Gibbs energy as:

$$\Delta=\boldsymbol{\sigma}:\dot{\boldsymbol{\varepsilon}}-\rho\dot{\psi}-\rho\dot{\theta}s=-\dot{\boldsymbol{\sigma}}:\boldsymbol{\varepsilon}-\rho\dot{g}-\rho\dot{\theta}s \tag{8}$$

From the relationship between the Gibbs energy and the compliance tensor of damaged material (consequently the damage effect tensor), given by equation (7), the rate of damage induced dissipation can be expressed in terms of rate of change of damage tensor as:

$$\Delta=\frac{1}{2}\boldsymbol{\sigma}:\mathbb{M}\left(\boldsymbol{\omega}\right):\mathbb{C}^{-1}:\frac{\partial\mathbb{M}\left(\boldsymbol{\omega}\right)}{\partial\boldsymbol{\omega}}:\boldsymbol{\sigma}:\dot{\boldsymbol{\omega}}\geq 0 \tag{9}$$

The dissipation rate (9) is determined by the definition of the damage effect tensor and the rate of change of damage tensor. Current model development utilises the damage effect tensor given in (2) and (3) and defines the damage in the principle direction from the parameters that controls the evolution of particular damaging modes. Namely, due to the pronounced heterogeneity/anisotropy of composite materials, a number of internal damage parameters can be defined in order to represent distinct damaging and failure modes, such as: tensile damage parameter, shear damage parameter, the interface damage parameter etc., see for instance [10]. Evolution of these parameters is then defined in the separate constitutive laws. This approach is used in definition of damage evolution in the constitutive model proposed in this work.

Damage evolution is modelled by using a modified Tuler-Bucher criretion [11]. Originally, Tuler and Bucher proposed a criterion for failure in a general form:

$$\phi=\int_{0}^{t_{cr}}f\left(\sigma\left(t\right)\right)dt \tag{10}$$

where: f can be any convenient function of stress, usually $(\sigma-\sigma_0)^{\lambda}$, σ_0 is a threshold stress below which no failure occurs and t_{cr} is time to failure. The method was originally proposed for unidirectional loading. In order criterion to be applied to the orthotropic material and three dimensional loading conditions, an effective value for the stress is utilised. Delamination is modelled by an in-plane criterion based on the out of plane (through thickness) normal stress component. The functions $f(\sigma(t))$ are normalized with the corresponding member of the material stiffness tensor, so that the evolution laws of the damage parameters are defined as:

$$\dot{\omega}=\dot{\omega}(\omega,\sigma)=\Omega_{\omega}\left(\frac{\sigma}{C_m(1-\omega)}-\frac{\sigma_{CR}}{C_m}\right)\left\langle\frac{\sigma}{C_m(1-\omega)}-\frac{\sigma_{CR}}{C_m}\right\rangle \tag{11}$$

$$\dot{\omega}_{del}=\dot{\omega}_{del}(\omega,\sigma)=\Omega_{del}\left(\frac{\sigma_{33}}{C_{33}(1-\omega_3)}-\frac{\sigma_{CRdel}}{C_{33}}\right)\left\langle\frac{\sigma_{33}}{C_{33}(1-\omega_3)}-\frac{\sigma_{CRdel}}{C_{33}}\right\rangle \tag{12}$$

where Ω_{ω}, Ω_{del} are material parameters determined by the time to failure, σ_{CR} and σ_{delCR} are critical effective stress and critical out of plane stress, C_m and C_{33} are maximum in-plane and through the thickness stiffness member, respectively. The brackets $\langle\ \rangle$ denote a Heaviside function (equal to one for the positive values of the expression within the brackets and zero for the negative values of the expression within the brackets).

The proposed damage model was implemented into the LLNL code DYNA3D [3] and coupled with an orthotropic elastic constitutive model and the Mie Gruneisen EOS, as detailed in [1].

3 Simulation results

Thermoelastic-damage model for composites was validated against the experimental data obtained in the sphere impact tests, performed at the range of impact velocities from 194 m/s to 1219 m/s. These test data allowed for validation of the model performance in the simulations of different failure mechanisms induced by the impact loadings, starting from the target ballistic limit to the extremely high loading rates, where the damage and failure are dominated by strong shock wave propagation. In addition, experimental trials, described in detail in [4], examined the effects of target thickness and layup onto the material response when exposed to the high velocity impact loading. Therefore, two woven CFRP target plates were used in the impact trials: 6 mm and 12 mm thick plates, which comprised 16 and 32 plies, respectively. The former was made of an asymmetric layup, which is illustrated in the Figure 4. In all test cases, the projectile was annealed SS304 stainless steel sphere, 12 mm in diameter, with the isotropic material properties.

Post processing of the target plates after the impact was done by using two non-destructive methods: X ray computed tomography (XCT) [12] and ultrasonic C-scan. The XCT was utilized for imaging the samples after the impacts at 194 m/s and 354 m/s. The images of the front plies and the specimens' cross sections with relevant parameters of damage are shown in Figure 1 and Figure 2, respectively. The photographs of delamination zones in the front and the rear face of the 12 mm thick specimen after the impact at 1219 m/s are shown in Figure 3.

The delamination area size and the diameter of the hole in this specimen were obtained from the C scans and these results are reported below in the Table 1.

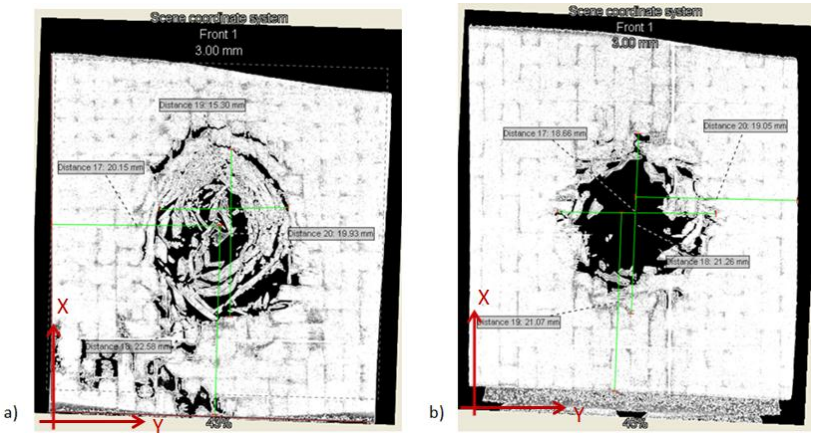

Figure 1. XCT parallel to the XY plane at 3 mm from the impact surface [12]; 6mm thick CFRP plates; impact velocity: a) 194 m/s b) 354m/s

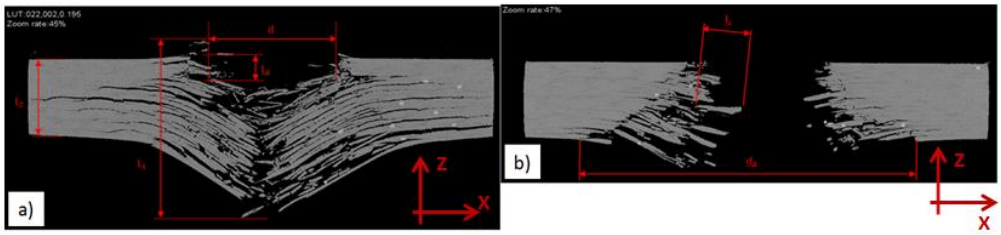

Figure 2. XCT parallel to the XZ plane through the impact point [12]; 6mm thick CFRP plates; impact velocity: a) 194 m/s b) 354m/s

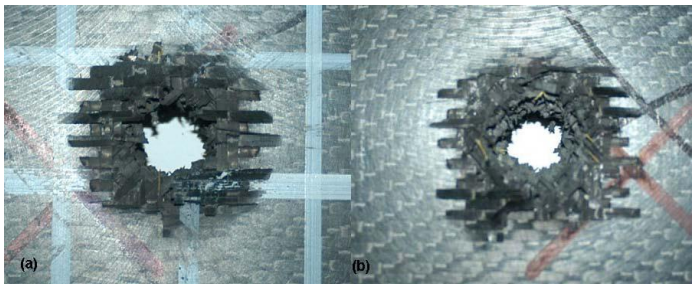

Figure 3. Damage distribution for 12mm thick CFRP plate [4], impact velocity 1219 m/s: (a) impact face and (b) rear face

The finite element model of a quarter of the sphere impact test at 6 mm thick target plate is shown in Figure 4, where two perpendicular symmetry planes through the normal impact axis were defined in terms of appropriate boundary conditions. Since the high velocity impact induced local effects, in order to reduce the computational costs, the dimensions of the FE model of the target plate were not the same as the dimensions of the real specimens, but were chosen in a way that boundary conditions were not affecting the numerical results. A quarter of the target plate was modelled by 96000 solid elements with one integration point, and a quarter of the sphere projectile was modelled with 4864 solid elements. The plate was modelled as a quasi-orthotropic material, with three solid elements per thickness in order to capture the delamination properly. The material properties of CFRP and Mie Grüneisen EOS data used in all simulations were taken from [1]. The contact algorithm used in the

simulations is Slide surfaces with Adaptive New Definitions (SAND), which is available in DYNA3D as contact type 11.

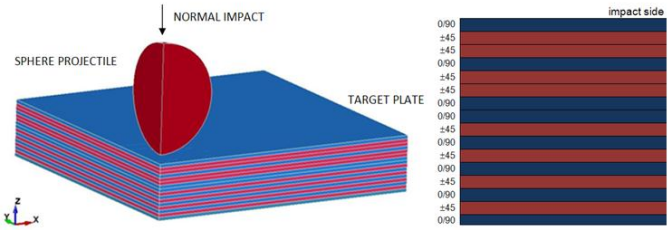

Figure 4. FE model of a quarter of the sphere impact test onto woven CFRP composite target

The area of damaged material of each ply, observed from the XCT scans after the impact at 194 m/s and 354 m/s, was elliptical in shape as illustrated in the Figure 1. This shape is a consequence of material orthotropy and was predicted well by numerical model. Comparison of the size of the damage area, calculated from the numerically obtained and experimentally observed data, for each ply through the target thickness, for the two impact velocities are illustrated in Figure 5 and Figure 6. The simulation results agree well with the experimental observations.

For the lower impact velocity, where the petalling is a dominant failure mode, the size of the damaged area decreases from the top to the bottom plies, as illustrated in Figure 2a and Figure 5. The numerical model only underestimated the size of the damage area at the back of the target plate. This can be attributed to the quasi-orthotropic equivalent composite properties, which made the model stiffer in the fibre directions (tensile fibre failure is dominant failure mechanism in rear plies of the target plate).

The post-impact XCT results for impact at 354 m/s, with a dominant shear plugging failure mode, show that size of the damaged area is increasing from the top to the bottom plies, resulting in a conical profile of the hole and the conical shape of the damage zone in the target cross section (see Figure 2b and Figure 6). This was also observed in the simulation results, and the damage distribution obtained in the numerical simulations 50μs after the impact is shown in Figure 7. Damage areas calculated from the numerical results agree well with the experimental data, as illustrated in Figure 6.

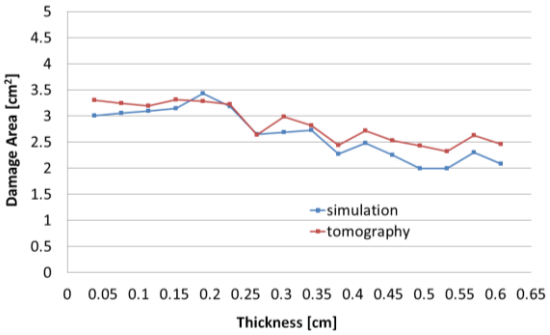

Figure 5. Damage area calculated from simulation results and tomography data for the normal impact at 194m/s

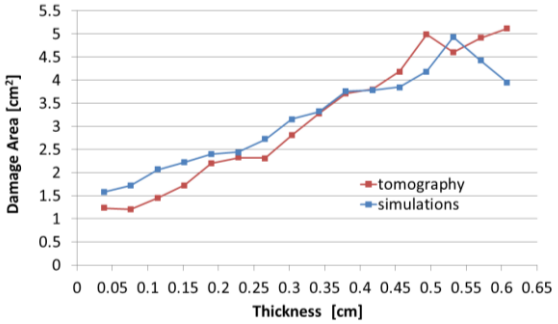

Figure 6. Damage area calculated from simulation results and tomography data for the normal impact at 354m/s

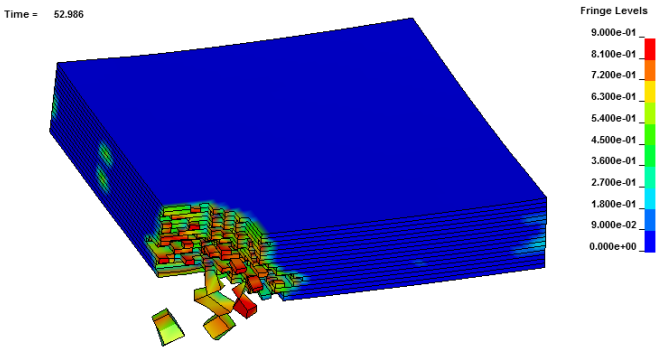

Figure 7. Damage distribution in the 6mm thick CFRP obtained in the simulation of normal impact at 354m/s; time 50μs after impact

The model performance in the simulation of the high velocity impact tests is illustrated by the results for the impact at 12mm thick target plate at impact velocity of 1219m/s. The hole and the damage area in the cross section of the target plate had an hourglass shape, with the wide damage (delamination) zone in the front and rear plies of the target plate (see Figure 3). The validation of the numerical model was based on the measurements of the diameter of the hole and diameter of the damage zone in the front and rear face in two perpendicular (in-plane) directions. The comparison of the numerical and experimental data is given in Table 1. The numerical results compare well with the experiments: 1) simulations captured hourglass shape of delaminated zone in the cross section of the target plate; 2) elliptical shape of the damage zone of each ply obtained in the simulations; 3) bigger delamination zone in the rear plies relative to the front plies; 3) average diameter of the hole calculated from the numerical results differs below 7% from the experimentally obtained values; 4) numerically obtained size of delamination zone at the rear ply is within 8% of the experimental data.

Sample	thickness [mm]	Impact velocity [m/s]	x_1 [mm]	x_2 [mm]	Impact face y_1 [mm]	Impact face y_2 [mm]	Rear face y_1 [mm]	Rear face y_2 [mm]
Simulations	12	1219	10.8	12.0	43.5	37.9	48.0	42.0
C scan C-3	11.9	1219	11.6	12.8	42.8	35.1	44.6	40.7
Difference	-	-	6.9	6.25	1.6	7.97	7.6	3.1

Table 1. Simulation results and C-scan measurements for the hole diameter and dimensions of the delamination zone for the impact at 12 mm thick CFRP at 1219 m/s

4 Summary

This paper describes a part of the validation process of the thermoelastic damage model proposed for the orthotropic materials including woven composites. This includes modelling of three sphere impact tests at 194, 354 and 1219 m/s. The post-impact extent of damage in the samples was determined using X ray tomography and ultrasonic C-scans and compared with the corresponding numerical results. The comparison showed that the model is capable of accurately predicting damage distribution and extent in plane and through thickness, especially for the high velocities, when the shock wave propagation significantly influenced the material response.

References

[1] Vignjevic R., Campbell J.C., Bourne N.K., Djordjevic N. Modelling shock waves in orthotropic elastic materials. *Journal of Applied Physics*, **104 (4)**, (2008).

[2] Hansen N. R., Schreyer H. L. A thermodynamically consistent framework for theories of elastoplasticity coupled with damage. *International Journal of Solids and Structures*, **31 (3)**, pp. 359-389 (1994).

[3] Jerry I.L. *DYNA3D User manual*. Methods Development Group – Mechanical Engineering, Lawrence Livermore National Laboratory (1998).

[4] Hazell P.J., Cowie A, Kister G, Stennett C, Cooper G.A. Penetration of a woven CFRP laminate by a high velocity steel sphere impacting at velocities of up to 1875 m/s, *International Journal of Impact Engineering*, **36**, pp. 1136-1142 (2009).

[5] Cordebois J. P., Sidoroff F. Anisotropic Damage in Elasticity and Plasticity. *Journal de mecanique theorique et appliquee*, , pp. 45-59 (1980).

[6] Kachanov L. M. Time of the rupture process under creep conditions. *Ivz Akad Nauk SSR Otd Tech Nauk*, **8**, pp. 26-31 (1958).

[7] Krajcinovic D. *Damage mechanics*. Elsevier, Amsterdam; New York (1996).

[8] Carol I., Rizzi E., Willam K. On the formulation of anisotropic elastic degradation I. Theory based on a pseudo-logarithmic damage tensor rate. *International Journal of Solids and Structures*, **38 (4)**, pp. 491-518 (2001).

[9] Malvern L. E. *Introduction to the mechanics of a continuous medium*, Prentice-Hall, Englewood Cliffs; London (1969).

[10] Naboulsi S. K., Palazotto A. N. Thermodynamic damage model for composite under severe loading. *Journal of Engineering Mechanics*, **126 (10)**, pp. 1001-1011 (2000).

[11] Tuler F.R., Bucher B.M. A criterion for the time dependence of dynamic fracture, *International Journal of Fracture Mechanics*, **4 (4)**, pp. 431-437 (1968).

[12] Penumadu D., Woven CFRP Composite Materials Damage from Steel Sphere Impact: Visualization and Analysis Using X-ray Micro CT, *X-ray CT Experimental data for the ELRIPS project*, University of Tennessee, (2010).